PRINT ISSN 1119-8362
Electronic ISSN 2659-1502

Full-text Available Online at
https://www.ajol.info/index.php/jasem
http://www.bioline.org.br/ja

J. Appl. Sci. Environ. Manage.
Vol. 27 (6) 1083-1091 June 2023

Effects of Preparation Conditions on Surface Properties and Yields of Periwinkle Shell Activated Carbon

OYEDOH, EA; EKESIOBI, UU

Department of Chemical Engineering, Faculty of Engineering, University of Benin, Benin-City, Nigeria

**Corresponding Author Email: egheoyedoh@uniben.edu*
Co-author Email: ekesiobi.uche@gmail.com

ABSTRACT: This study explored the potential of periwinkle shells as precursor material for activated carbon preparation. The periwinkle shell was activated using the potassium hydroxide method. The periwinkle shell activated carbons prepared were characterized in terms of physico-chemical properties, functional groups, and yield and surface characteristics. The central composite design of response surface methodology was used for analysis and optimization of carbonization conditions of the periwinkle shell. The carbonization conditions considered and their range of values are carbonization temperature of 300 to 700℃ and carbonization time of 30 to 180 mins. The FTIR analysis showed the presence of stretching vibration bands such as carbonate ion, aliphatic and heterocyclic N-H. The optimum conditions of the periwinkle shell carbonization carbon preparation are carbonization temperature of 536.38℃ and carbonization time of 82.09 mins. These conditions gave maximum responses of PSBC's yield percentage of 95.15%, surface area of 71.53 m^2/g and porosity of 36.70. The R^2 values obtained were very high for each response; 99.47%, 99.98% and 97.77% for PSBC's yield, surface area and porosity respectively indicating that the results of experimental studies were in perfect agreement with those suggested from model. Periwinkle shells were found to be an efficient precursor material for activated carbon preparation with a very high yield as well as excellent surface characteristics.

DOI: **https://dx.doi.org/10.4314/jasem.v27i6.6**

Cite this paper as: OYEDOH, E.A; EKESIOBI, U. U. (2023). Effects of Preparation Conditions on Surface Properties and Yields of Periwinkle Shell Activated Carbon. *J. Appl. Sci. Environ. Manage.* 27 (6) 1083-1091

Dates: Received: 19 May 2023; Revised: 04 June 2023; Accepted: 09 June 2023 Published: 30 June 2023

Keywords: Periwinkle shell; activated carbon; carbonization conditions; surface properties; optimization

Together with pollution levels, industry growth, and urbanization, there is an increasing demand of water treatment technologies. Technologies involving activated carbon have been identified as credible water treatment schemes. However, the expensive cost of raw resources restricts the product's rapid spread (Ahmad *et al*., 2020). The percentage consumption of activated carbon has gradually increased as contemporary technology has advanced. Due to this, innovators are searching for the various ways in which it can be obtained and used. In recent times, the production of activated carbon from biomass, especially agricultural wastes, has gained enormous interest as against the initial methods from petroleum or coal. Recently, it is now being produced from wood, waste cocoa pod walnut shells, groundnut shells, coconut shells, snail shells, periwinkle shells etc (Mohd Iqbaldin *et al*., 2013). The exceptional physico-chemical characteristics of activated carbon, enable it to be used in a variety of applications. Catalysis, gas purification, chemical storage and purification, and electrode material for energy storage systems are only a few uses for activated carbon. High surface area, flexible pore size and volume, chemical inertness, and stability are among the qualities of activated carbon (Abioye and Ani, 2015; Banerjee *et al*., 2020). Most commercial activated carbons are expensive and harmful to the environment because they are mostly produced using coal and petroleum as precursors. As a result, more emphasis is being placed on biomass precursors, which are less expensive, more readily available, renewable, structurally porous, and

**Corresponding Author Email: egheoyedoh@uniben.edu*

environmentally friendly (Abbas and Ahmed, 2016; Abioye and Ani, 2015; Farma *et al*., 2013). Periwinkles (*T. fuscautus)* are marine snails that belong to the shellfish family *Gastropod mollusc*. In Nigeria, the *T. fuscautus* species is the most abundant and it is commonly found in the Niger-Delta region in locations along the shore. Periwinkle shell is substantial and heavy (Badmus and Audu, 2009) and is a by-product obtained after the edible part of the periwinkle shellfish is removed (Eziefula *et al*., 2020). Periwinkle shell wastes are commonly piled in open fields and landfills, resulting in a foul odor, ugly appearance, and the development of disease-carrying organisms (Morris *et al*., 2019). In order to mitigate the environmental impact of the shells several alternative uses have being developed over time. One of which is the production of activated carbon from periwinkle shells. Periwinkle shells provide a very cheap, sustainable and rich source of carbon. Also, compared to commercial activated carbon (CAC), the production process for periwinkle shell activated carbon (PSBC) is more eco-friendly (Banerjee *et al*., 2020; Wang *et al*., 2017). The properties of the activated carbon produced is dependent on number of factors. Banerjee *et al*. (2020) stated that factors such as; the type of biomass precursor used, carbonization temperature, carbonization time, impregnation rate, the type of functional group, content of heterofoam, extent of graphitization have a way of affecting the properties of the activated carbon. In order to produce activated carbon with the best surface properties, these factors have to be optimized. Activated carbon synthesis using the "one factor at a time" method does not show the interaction between factors (Ahmad *et al*., 2020) and hence the need for optimization. In this study, the effects of preparation conditions on the surface properties and yields of periwinkle shell activated carbon were investigated.

MATERIALS AND METHODS

Sample collection and preparation: Periwinkle shells were collected as waste in a local market in Benin City, Edo State, Nigeria. The shells were thoroughly washed with warm water to remove soil particles and other undesired materials. The shells were then sun-dried to remove excess water and packed into a polyethylene for further processing in the laboratory.

Carbonization and carbonization process: The carbonization and carbonization of the periwinkle shells was done using method by Mohd Iqbaldin *et al*. (2013). Periwinkle shells of 30.0 grams (w_1) were weighed into 13 crucibles and placed in an electric muffle furnace over the time and temperature of carbonization stipulated for each run by the experimental design (Table 1). After heating, the periwinkle shells were left to cool in a desiccator and re-weighed again and noted as w_2 for each run. Each run was grinded and sieved through a 250 µm sieve then added to a 250 ml beaker and labeled. For the carbonization process, 60 ml of 0.5 M KOH was added to each run and subjected to heat of about 105^0 C in an air-drying oven for 2 hours. The process of washing out was carried out to neutralize the KOH from the periwinkle shell solution. The process involved adding water and drops of 4% sulfuric acid (H_2SO_4) to the solution and filtering using a filter paper and funnel until neutralization is attained. After neutralization and filtration, each run was dried in the oven at the temp of 110^{o}C. The yield of activated carbon is usually defined as final weight of activated carbon produced after carbonization, washing, and drying, divided by initial weight of raw material; both on a dry basis (Prahas *et al.*, 2008). The percentage yield of activated carbon produced was determined using the Equation (1).

$$Yield\ (\%) = \frac{w_2}{w_1}\ x\ 100\ \% \qquad (1)$$

Where w_1 is the initial weight of periwinkle shell before carbonization and w_2 is the final weight of the periwinkle shell after carbonization.

Determination of surface area by iodine number method: About 10 ml of 5% HCl solution was added to 1.0 gram of the activated carbon sample and boiled for 60 seconds and allowed to cool. Thereafter, 20 ml of 2.1 M of iodine solution was added to each of the mixtures and then subjected to intensive shaking using an orbital shaker for 5 minutes. Then, 0.2 ml of starch solution was added in drops to 10 ml of each HCl-Iodine solution mixture until it turned blue-black.The HCl-Iodine-starch solution mixture was titrated against 0.1 M sodium thiosulfate solution. The titer volumes obtained were recorded for each titration. Blank titration was also carried out without the sample to determine the blank titer volume. To determine the surface area, the iodine number was first calculated using Equation (2);

$$IN = \frac{V_b - V_s}{m}\ x\ N\ x\ 126.9 \qquad (2)$$

Where IN represents the iodine number, m is mass of sample, N is normality (0.1N), V_b is the titre volume of blank, V_s is the titre volume of sample.

The surface area (S_i) was calculated using the Equation (3);

$$Si = \frac{IN\ x\ 10^{-5}}{mi}\ x\ N\ x\ Wi \qquad (3)$$

Where IN is the iodine number, *molecular weight of iodine* (m_i) = 126.92 g/mol, Avogadro number ***(N)*** =

6.023×10^{23} mol^{-1} and surface area occupied by one adsorbate in the complete monolayer pack (w_i) = 0.2096×10^{-18} m^2

Determination of porosity: To determine the porosity, 10 ml of each sample was measured into a measuring cylinder and 10 ml of water was added to each sample. Each sample was filtered to collect the volume of water that could pass through the sample. Porosity was calculated for using Equation (4);

$$Porosity = \frac{V_l}{V_s} x\ 100\ \% \qquad (4)$$

V_l = volume of liquid that penetrates into the sample and V_S = volume of sample

Design of experiment: A statistical model for the activated carbon production process was design using the Central Composite Design (CCD) for response surface methodology. Two-independent variables were investigated in these studies for the preparation of AC; they are: X_1, carbonization temperature (°C) and X_2, carbonization time (mins). There are 4 factorial points, 4 axial points and 5 replicates at the center points, indicated by a total of 13 experimental runs for the production process., as calculated by Equation (5);

$$Total\ number\ of\ experiments\ (N) = 2^n + 2n + nc = 2^2 + 2 \times 2 + 5 = 13 \quad (5)$$

Where *n* is the number of factors, nc is the number of center points (five replicates)

The reproducibility of the data and the experimental error were verified using the center points The variables were coded in the (-1, 1) interval, with -1 and +1 representing the low and high levels, respectively. The axial points are usually located at (±α, 0, 0), (0, ±α, 0), and (0, 0, ±α), where α is the fixed at 1.414. The coded and actual values for the central composite design are shown in Table 1.

The three responses are activated carbon yield (Y_1), surface area (Y_2) and porosity (Y_3). Each response was used to develop an empirical model which correlated the response to the variables using a second- degree polynomial Equation (6) as follow (Ahmad *et al*., 2017):

The influence of a single factor is represented by the coefficient with one factor, but the interaction of two factors and quadratic effects are represented by the coefficient with two factors and those with second-order terms. The feature of desirability was applied using Design Expert software version 11.1.2.0 (STAT-EASE Inc., Minneapolis, USA) to reach a compromise between the results. The coefficient of determination and analysis of variance (ANOVA) were used to evaluate the suitability of the derived model for predicting yield, surface area and porosity, as well as the significance levels of the linear, interaction and quadratic factors (Dargahi *et al*., 2021).

Table 1: Coded and Actual values for the factors of Central Composite Design

Independent Variables	Symbols	Coded and Actual Level				
		-α	-1	0	+1	+α
Carbonization temperature (°C)	X_1	300	358.58	500	641.42	700
Carbonization time (mins)	X_2	30	51.97	105	158.03	180

$$Y = bo + \sum_{i=1}^{n} bixi + \left(\sum_{i=1}^{n} biixi\right)^2 + \sum_{i=1}^{n-1} \sum_{j=1+i}^{n} bijxixj \quad (6)$$

Where Y stands for the predicted response, bo = constant coefficient, bi = linear coefficients, bij = interaction coefficients, bii = quadratic coefficients and xi and xj stand for coded values of the activated carbon production variables.

RESULTS AND DISCUSSION

Fourier transform infrared (FTIR) spectra: Oxygen containing surface functional groups plays important role in influencing the surface properties and adsorption behavior of activated carbons (Dawood and Sen, 2014). These groups can be formed during carbonization process or can be introduced by oxidation after preparation of activated carbon. The FTIR spectra obtained for the prepared adsorbent is given in Figure 1. The sample showed three major absorption bands in the region 1600 – 1400 cm^{-1}. The strong band around 1435 cm^{-1} refers to the stretching vibrations of Carbonate ion (CO_3^{-2}) bonds which is often found in activated carbons. Similarly, the weak peak seen at 3395.60477 cm^{-1} has been assigned to stretching vibrations of aliphatic primary amine (N – H) bonds. The summary of the results is as presented in Table 2.

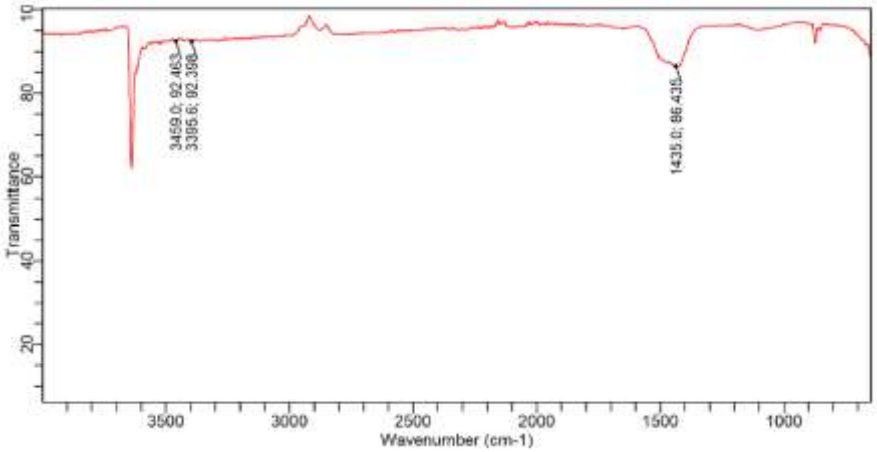

Fig 1: FTIR Spectrum of PSBC

Table 2: Result of Spectrum peaks of PSBC.

Peak No.	Wavenumber (cm^{-1})	Intensity	Functional Group	Description
1	1435.0	86.435	Carbonate ion (CO_3^{-2})	Strong stretched
2	3395.6	92.398	Aliphatic primary amine (N – H)	Weak stretched
3	3459.0	92.463	Heterocyclic amine (N – H)	Weak stretched

A
nalysis of results: Design Expert Software was used to analyze the experimental data. Investigation was carried out on linear interaction, two factor interaction and quadratic models to determine the best statistically significant model and the model that best describes the relationship between the inputs and the response. The models were selected based on the highest order polynomials where the additional terms were significant and the model, not aliased. The model summary statistics of yield, surface area and porosity responses is shown in Tables 3, 4 and 5 respectively.

Table 3: Model Statistics for Yield (Y_1) Response

Source	Std. Dev.	R^2	Adjusted R^2	Predicted R^2	PRESS	
Linear	0.5508	0.9205	0.9045	0.8323	6.40	
2FI	0.3607	0.9693	0.9591	0.9361	2.44	
Quadratic	**0.2568**	**0.9879**	**0.9792**	**0.9379**	**2.37**	**Suggested**
Cubic	0.2899	0.9890	0.9736	0.5644	16.62	Aliased

Table 4: Model Statistics for Surface Area Response (Y_2)

Source	Std. Dev.	R^2	Adjusted R^2	Predicted R^2	PRESS	
Linear	28.45	0.0116	-0.1861	-0.6364	13404.18	
2FI	29.96	0.0135	-0.3154	-1.2021	18037.97	
Quadratic	**0.4315**	**0.9998**	**0.9997**	**0.9991**	**7.54**	**Suggested**
Cubic	0.3611	0.9999	0.9998	0.9973	22.27	Aliased

Table 5: Model Statistics for Porosity Response (Y_3)

Source	Std. Dev.	R^2	Adjusted R^2	Predicted R^2	PRESS	
Linear	**0.8016**	**0.9777**	**0.9732**	**0.9544**	**13.12**	**Suggested**
2FI	0.8315	0.9784	0.9711	0.9246	21.67	
Quadratic	0.9317	0.9789	0.9638	0.8685	37.83	
Cubic	0.4880	0.9959	0.9901	0.9455	15.67	Aliased

$$Y_1 = 94.76 - 1.32x_1 - 1.63x_2 - 0.6825x_1x_2 + 0.0484x_1^2 - 0.3066x_2^2 \quad (7)$$
$$Y_2 = 78.48 - 0.986x_1 + 3.30x_2 + 1{,}98x_1x_2 - 32.01x_1^2 - 15.76x_2^2 \quad (8)$$
$$Y_3 = 35.49 + 5.88x_1 + 0.7135x_2 \quad (9)$$

It shows that quadratic model was generated by RSM as it was statistically significant for yield (Y_1) and surface area (Y_2) responses. Meanwhile, for porosity (Y_3) response, linear model was selected. The coefficient with one factor represents the particular factor effect only, whilst the coefficients with two

factors and the second-order term represent the interaction of two factors and the quadratic effect, respectively. The final empirical formula models for the responses in terms of coded factors are represented by Equations (7), (8) and (9) respectively. Correlation coefficient, R^2 value was very crucial for validation of the model developed. The R^2 values for Equations (7), (8) and (9) are 0.9879, 0.9998 and 0.9777, respectively. These results indicate 98.79%, 99.98% and 97.77% of the total variation in the PSBC yield, surface area and porosity correlation between the experimental and predicted values respectively. These high R^2 values show that the predicted responses were near to the experimental values indicating that the models are adequate for correlating with experiment data hence validating the models and results obtained. The complete design matrix for preparing PSBC and responses obtained is given in Table 6.

Analysis of variance (ANOVA): Through the ANOVA, the models' significance and adequacy were demonstrated. A p-value less than 0.05 shows that the outcome is not random and that the factor or term has a substantial or significant impact on the response (Ahmad *et al.*, 2017). Tables 7, 8 and 9 shows the results of the ANOVA for the quadratic PSBC yield, surface area and porosity models respectively. From Table 7, the large model F-value of 114.26 and small P-values less than 0.05 (0.0001) implied the model is highly significant. In this case the effects of carbonization temperature (X_1), carbonization time (X_2), interaction of carbonization temperature and time (X_1X_2) and the quadratic factor X_2^2 were significant on the yield of PSBC. Whereas, the quadratic factor (X_1^2) was insignificant on the yield of PSBC. The Lack of Fit F-value of 2.41 implied the Lack of Fit was not significant relative to the pure error. Non-significant lack of fit is good. The Predicted R^2 of 0.9379 was in reasonable agreement with the Adjusted R^2 of 0.9792; i.e. the difference is less than 0.2. Adequate precision measures the signal to noise ratio. A ratio greater than 4 is desirable. The adequate precision ratio of 33.779 was obtained, thus indicative an adequate signal.

Table 6: Experimental design matrix including experimental and predicted responses

Run	Factors				Responses					
	Carbonization temperature (ºC)		Carbonization time (mins)		Y_1 Yield (%)		Y_2 Surface area (m^2/g)		Y_3 Porosity (%)	
**/	X_1	Actual	X_2	Actual	Actual	Predicted	Actual	Predicted	Actual	Predicted
1	-1	358.58	1	158.03	95.00	94.88	33.14	33.01	30.90	30.32
2	0	500	1.41	180	91.77	91.85	51.74	51.62	37.20	36.50
3	1	641.42	1	158.03	90.97	90.87	34.57	35.00	41.00	42.09
4	1.41	700	0	105	92.83	92.99	13.66	13.06	44.47	43.81
5	0	500	0	105	94.91	94.76	78.13	78.48	35.72	35.49
6	-1.41	300	0	105	96.53	96.73	15.66	15.85	26.10	27.17
7	0	500	0	105	94.97	94.76	78.72	78.48	35.72	35.49
8	0	500	-1.41	30	96.17	96.45	42.59	42.30	33.80	34.48
9	-1	358.58	-1	51.97	97.03	96.77	30.39	30.38	30.00	28.89
10	0	500	0	105	94.50	94.76	78.39	78.48	35.50	35.49
11	0	500	0	105	94.60	94.76	78.81	78.48	34.53	35.49
12	0	500	0	105	94.83	94.76	78.36	78.48	35.42	35.49
13	1	641.42	-1	51.97	95.73	95.49	23.90	24.45	41.00	40.66

Table 7: ANOVA for quadratic model of yield of PSBC

Source	Sum of squares	df	Mean square	F-value	p-value
Model	37.68	5	7.54	114.26	< 0.0001*
X_1 - Carbonization temperature	13.95	1	13.95	211.43	< 0.0001*
X_2 - Carbonization time	21.17	1	21.17	320.88	< 0.0001*
X_1X_2	1.86	1	1.86	28.25	0.0011*
X_1^2	0.0163	1	0.0163	0.2468	0.6346
X_2^2	0.6540	1	0.6540	9.92	0.0162*
Residual	0.4617	7	0.0660		
Lack of fit	0.2970	3	0.0990	2.41	0.2079
Pure error	0.1647	4	0.0412		
Corrected total	38.15	12			
Standard deviation (m^2/g)	0.2568				
Mean (m^2/g)	94.60				
C.V (%)	0.2715				
R^2	0.9879				
Adjusted R^2	0.9792				
Predicted R^2	0.9379				
Adequate precision	33.7789				

**=statistically significant*

The ANOVA for quadratic model for surface area is shown in Table 8. The large m**odel F-value** of 8799.22 and small model p-value of < 0.0001 implied the model is highly significant. The observed **P-values** less than 0.05 indicate model terms are significant. In this case X_1, X_2, X_1X_2, X_1^2, X_2^2 are significant on the surface area of PSBC. The **Lack of Fit F-value** of 4.24 was not significant relative to the pure error. The **Predicted R²** of 0.9991 is in a good agreement with the **Adjusted R²** of 0.9997. **Adequate precision** ratio of 223.197 indicate an adequate signal. The ANOVA for the linear model of PSBC porosity is shown in Table 9. The large m**odel F-value** of 218.77 implied the model is significant. **P-values** less than 0.05 indicate model terms are significant. In this case X_1 and X_2 are significant on the porosity of PSBC. The **Lack of Fit F-value** of 3.75 implied the Lack of Fit was not significant relative to the pure error. The **Predicted R²** of 0.9544 is in reasonable agreement with the **Adjusted R²** of 0.9732 and a**dequate precision** of 43.227 suggest an adequate signal.

Table 8: ANOVA for quadratic model of surface area of PSBC

Source	Sum of Squares	df	Mean Square	F-value	p-value
Model	8190.04	5	1638.01	8799.22	< 0.0001*
X_1 - Carbonization temperature	7.78	1	7.78	41.78	0.0003*
X_2 - Carbonization time	86.86	1	86.86	466.59	< 0.0001*
X_1X_2	15.68	1	15.68	84.24	< 0.0001*
X_1^2	7129.77	1	7129.77	38300.44	< 0.0001*
X_2^2	1728.20	1	1728.20	9283.73	< 0.0001*
Residual	1.30	7	0.1862		
Lack of fit	0.9916	3	0.3305	4.24	0.0982
Pure error	0.3115	4	0.0779		
Corrected total	8191.34	12			
Standard deviation (m^2/g)	0.4315				
Mean (m^2/g)	49.08				
C.V (%)	0.8791				
R^2	0.9998				
Adjusted R^2	0.9997				
Predicted R^2	0.9991				
Adequate precision	223.197				

**=statistically significant*

Table 9: ANOVA for linear model of porosity of PSBC

Source	Sum of Squares	df	Mean square	F-value	p-value
Model	281.13	2	140.56	218.77	< 0.0001*
X_1 - Carbonization temperature	277.06	1	277.06	431.21	< 0.0001*
X_2 - Carbonization time	4.07	1	4.07	6.34	0.0305*
Residual	6.43	10	0.6425		
Lack of fit	5.46	6	0.9092	3.75	0.1107
Pure error	0.9697	4	0.2424		
Corrected total	287.55	12			
Standard deviation (m^2/g)	0.8016				
Mean (m^2/g)	35.49				
C.V (%)	2.26				
R^2	0.9777				
Adjusted R^2	0.9732				
Predicted R^2	0.9544				
Adequate precision	43.2268				

**=statistically significant*

Parity plots: The experimental and predicted values shown in Table 6 were plotted to analyze the correlation between them as shown in Figure 2(a), (b) and (c) for yield, surface area and porosity respectively. It is observed from the plots that the data points are distributed near the straight line. This further indicates that the models specified for each response could be employed as the significant model for the predicting responses over the independent input variables.

Effects of interaction of variables of PSBC yield, surface area and porosity: The effects of interaction of carbonization temperature and time on the yield, surface area and porosity of PSBC is given by the 3-dimensional response surface plots shown in Figure 3 (a), (b) and (c) respectively.

The 3-D response surface plot in Figure 3 (a) indicate that both carbonization temperature and carbonization time had substantial effect on the yield. However, the carbonization time had the highest effect on the percentage yield since it gave the highest F-value of 320.88. At 358.58ºC and 51.97 mins, the highest PSBC yield (97.03%) (Table 6) was achieved.

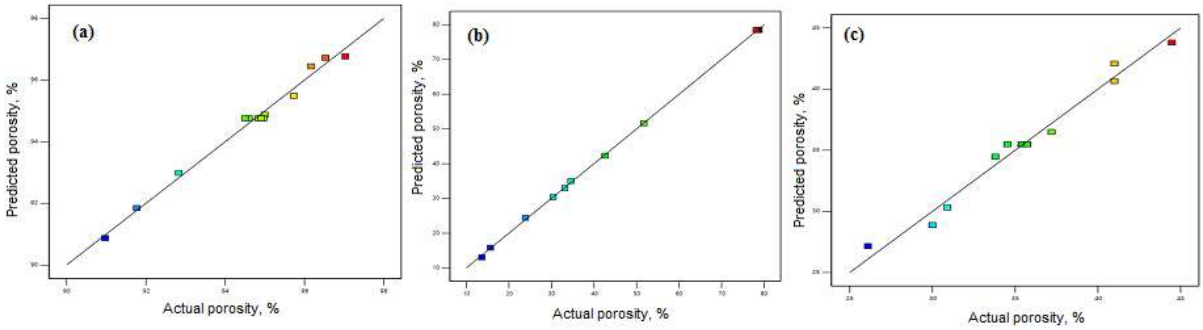

Fig 2: Predicted versus experimental values plot for (a) yield, (b) surface area and (c) porosity responses of PSBC

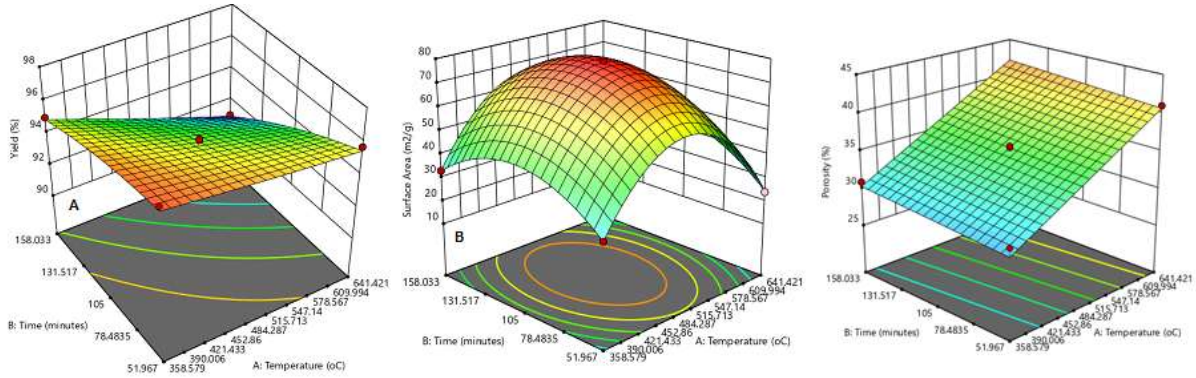

Fig 3: Response surface plots showing the effects on carbonization temperature and time on (a) yield, (b) surface area and (c) porosity of PSBC from the carbonization process**.**

It should be noted that these were the lowest values of the independent variables which may be due to an incomplete elimination of volatile matter and tar from the carbonization process (Ahmad *et al*., 2016) . These volatile matter and tar compounds added more weight to the PSBC, thus higher yield was obtained. Increasing the temperature causes the rate of reactions in C–CO_2 and C–KOH to also increase leading to decrease in carbon yield and increase in carbon "burn-off" by KOH (Ahmad *et al*., 2020; Liu *et al*., 2010). The PSBC yield continued to decrease gradually with increasing carbonization temperature and time. Similar trend was observed in the studies on optimization of preparation conditions for activated carbon from P*rosopis africana* seed hulls on batch adsorption studies of malachite green dye using rambutan seed activated carbon (Rahim and Garba, 2016). From Table 8, the F-value was indicative that the independent variables; carbonization temperature and carbonization time had significant effects on the surface area obtained. Activated time however, had the highest F-value (466.59). The values of surface area achieved ranged from 13.66 – 78.81 m^2/g. as presented in Table 8. It can be seen from the 3-D response surface of Figure 3 (b) that the surface area gradually increased with temperature up to a point and decreased with further temperature increment. When periwinkle shell particles are exposed to high carbonization temperatures over an extended period of time, the volatile chemicals in the inner half of the particle evaporate. This aids the periwinkle shell particles in acquiring deeper pores, resulting in a larger surface area. With higher carbonization temperatures, the surface area grows until it reaches a maximum point. Whereas a greater carbonization temperature is known to provide a large surface area for activated carbon, attempting to create excessively large pores will cause cell wall weakening. The mesopores were generated when many nearby micropores collapsed, reducing the surface area (Liu *et al*., 2018). The results of this study was in accordance to the influence of different chemical reagents on the preparation of activated carbons from bituminous coal and optimization of activated carbon preparation from cassava stem using response surface methodology on surface area and yield as reported by Hsu and Teng (2000) and Sulaiman *et al*. (2018). Considering the F-value in Table 9, it implied that both carbonization temperature and carbonization time influenced the porosity achieved. However, the most tangible effect was observed in the carbonization temperature. It had the highest F- value of 431.21 which greatly outweighs the F-value of 6.34 obtained for the carbonization time. The highest value of porosity (44.47%) was achieved at 700ºC and 105 mins (Table 9). From Figure 3 (c), the response surface plot showed an increase of

porosity with carbonization temperature and carbonization time. The increase in porosity with temperature can be attributed to the release of tars from cross-linked framework generated by KOH treatment (Prahas *et al*., 2008). This result was in accordance with the studies on the production of activated carbon from snail shell waste (*Helix pomatia*) and influence of different chemical reagents on the preparation of activated carbons from bituminous coal (Gumus and Okpeku, 2015; Hsu and Teng, 2000).

Optimization of activated carbon production process: The goal of the experiment was to determine the best production conditions for a high PSBC yield, as well as a large surface area and porosity. However, optimizing these three answers under the same condition was difficult due to the different interest zones of variables. Some runs had very high yield matched with low surface area and low porosity and vice versa, hence the need to find the optimum operating conditions to maximize all responses. Numerical optimization was performed using the Design Expert Software to apply the function of desirability to acquire a compromise between these three responses. Table 11 shows the optimal conditions for preparing PSBC that will maximize all responses.

Table 11: Optimum conditions for PSBC preparation

Temperature (℃)	Time (mins)	Yield (%)	Surface Area (m^2/g)	Porosity (%)	Desirability
536.38	82.09	95.15	71.53	36.70	0.707

Conclusions: This study employed response surface methodology to examine the influence of the effects of preparation conditions on the percentage yield, surface area and porosity of periwinkle shell activated carbon. It was found that periwinkle shell showed credible potential as a precursor for activated carbon preparation with high yield and surface properties. The quadratic and linear models developed for experimental designs and process optimization were found to be significant for predicting and understanding the responses as a function of the of process parameters.

REFERENCES

Abbas, AF; Ahmed, MJ (2016). Journal of Water Process Engineering Mesoporous activated carbon from date stones (*Phoenix dactylifera L*.) by one-step microwave assisted K_2CO_3 pyrolysis. *J. Wat. Process Engineer. 9:* 201–207.

Abioye, AM; Ani, FN (2015). Recent development in the production of activated carbon electrodes from agricultural waste biomass for supercapacitors: A review. *Renew. Sustain. Energy Rev. 52:* 1282–1293.

Ahmad, AA; Din, ATM; Yahaya, NKE; Khasri, A; Ahmad, MA (2020). Adsorption of basic green 4 onto gasified Glyricidia sepium woodchip based activated carbon: Optimization, characterization, batch and column study. *Arabian Journal of Chemistry*, *13*(8): 6887–6903.

Ahmad, MA; Afandi, NS; Adegoke, KA; Bello, OS (2016). Optimization and batch studies on adsorption of malachite green dye using rambutan seed activated carbon. *Desalination and Water Treatment*, *57*(45): 21487–21511.

Ahmad, MA; Afandi, NS; Bello, OS (2017). Optimization of process variables by response surface methodology for malachite green dye removal using lime peel activated carbon. *Applied Water Science*, *7*(2): 717–727.

Awokoya, K; Sanusi, R; Oninla, V; Ajibade, O (2016). Activated Periwinkle Shells for the Binding and Recognition of Heavy Metal Ions from Aqueous Media. *International Research Journal of Pure and Applied Chemistry*, *13*(4): 1–10.

Badmus, MA; Audu, TOK (2009). Periwinkle Shell: Based Granular Activated Carbon for Treatment of Chemical Oxygen Demand (COD) in Industrial Wastewater. *Canadian Journal Chemical Engineering*, 87: 69 – 77.

Dargahi, A; Samarghandi, MR; Shabanloo, A; Mahmoudi, MM; Nasab, HZ (2021). Statistical modeling of phenolic compounds adsorption onto low-cost adsorbent prepared from aloe vera leaves wastes using CCD-RSM optimization: effect of parameters, isotherm, and kinetic studies. *Biomass Conversion and Biorefinery*. DOI: 10.1007/s13399-021-01601-y

Dawood, S; Sen, TK (2014). *Review on Dye Removal from Its Aqueous Solution into Alternative Cost Effective and Non-Conventional Adsorbents*. Journal of Chemical and Process Engineering. 1: Article ID 104.

Eziefula, UG; Obiechefu, GC; Charles, ME (2020).

Use of periwinkle shell by-products in Portland cement-based materials: An overview. *International Journal of Environment and Waste Management*, *26*(3): 402–422.

Farma, R; Deraman, M; Awitdrus, A; Talib, IA; Taer, E; Basri, NH; Manjunatha, JG; Ishak, MM; Dollah, BNM; Hashmi, SA (2013). Preparation of highly porous binderless activated carbon electrodes from fibres of oil palm empty fruit bunches for application in supercapacitors. *Bioresource Technology*, *132:* 254–261.

Gumus, RH; Okpeku, I (2015). Production of Activated Carbon and Characterization from Snail Shell Waste. *Advances in Chemical Engineering and Science*, *05*(01): 51–61.

Hsu, LY; Teng, H (2000). Influence of different chemical reagents on the preparation of activated carbons from bituminous coal. *Fuel Processing Technology*, *64*(1): 155–166.

Liu, QS; Zheng, T; Wang, P; Guo, L (2010). Preparation and characterization of activated carbon from bamboo by microwave-induced phosphoric acid carbonization. *Industrial Crops and Products*, *31*(2): 233–238.

Liu, Y; Zhao, Y; Li, K; Wang, Z; Tian, P; Liu, D; Yang, T; Wang, J (2018). Activated carbon derived from chitosan as air cathode catalyst for high performance in microbial fuel cells. *J. Power Sources.* 378: 1–9.

Mohd Iqbaldin, MN; Khudzir, I; Mohd Azlan, MI; Zaidi, AG; Surani, B; Zubri, Z (2013). Properties of coconut shell activated carbon, Journal of Tropical Forest Science, 25(4): 497–503.

Morris, JP; Backeljau, T; Chapelle, G (2019). Shells from aquaculture: a valuable biomaterial, not a nuisance waste product. *Reviews in Aquaculture*, *11*(1): 42–57.

Olafadehan, OA; Jinadu, OW; Salami, L; Popoola, OT (2012). Treatment Of Brewery Wastewater Effluent Using Activated Carbon. *International Journal of Applied Science and Technology*, *2*(1): 165–178.

Prahas, D; Kartika, Y; Indraswati, N; Ismadji, S (2008). Activated carbon from jackfruit peel waste by H_3PO_4 chemical carbonization: Pore structure and surface chemistry characterization. *Chemical Engineering Journal*, *140*(1–3): 32–42.

Rahim, AA; Garba, ZN (2016). Optimization of preparation conditions for activated carbon from Prosopis africana seed hulls using response surface methodology. *Desalination and Water Treatment*, *57*(38): 17985–17994.

Sulaiman, NS; Hashim, R; Mohamad Amini, MH; Danish, M; Sulaiman, O (2018). Optimization of activated carbon preparation from cassava stem using response surface methodology on surface area and yield. *Journal of Cleaner Production*, *198:* 1422–1430.

Wang, J; Nie, P; Ding, B; Dong, S; Hao, X; Dou, H; Zhang, X (2017). Biomass derived carbon for energy storage devices. *J. Mat. Chem. A*, *5*(6): 2411–2428.